

Cercospora beticola toxins. Part 16. X-Ray diffraction analyses on microcrystals of three *p*-beticolins



Thierry Prangé,^{*,a} Alain Neuman,^a Marie-Louise Milat^b and Jean-Pierre Blein^b

^a *Chimie Structurale Biomoléculaire (URA-1430 CNRS), UFR Biomédicale, F-93017 Bobigny Cedex, France*

^b *Laboratoire de Phytopharmacie et Biochimie des Interactions Cellulaires, INRA-Université de Bourgogne, BV 1540, F-21034 Dijon Cedex, France*

The major yellow compounds extracted from the mycelium of *Cercospora beticola*, the beticolins, can be divided into two subgroups, the *o*- and the *p*-beticolins. It has been found that crystallogenesis conditions which allowed the X-ray analyses of the first subgroup are unsuccessful for the second. New conditions affording microcrystals for three *p*-beticolins, B1, B3 and B13 are described. Diffraction experiments have been performed on a synchrotron beam line; the results confirm the proposed structures for B1 and B3 and allow that of B13 to be elucidated.

Introduction

Cercospora beticola is a fungus responsible for the spot-leaf disease on sweet beets. It produces, in addition to the red cercosporin,¹ several yellow toxins that were named beticolins (Fig. 1). One of them was isolated and characterised in 1971 as CBT² (for *Cercospora beticola* toxin), but its chemical structure was not elucidated. A recent re-investigation of these toxins by X-ray analysis³⁻⁵ allowed the structures of three of the toxins (B0, B2 and B4) to be identified.³⁻⁵ The structure of a magnesium chelate named cebetin-B has also been reported independently,⁶ and has been found to be a dimer of the previously isolated CBT. Cebetin-B is the association of two subunits (cebetin-A or beticolin-1) joined together in a head-to-tail fashion around two magnesium ions. Following these initial determinations, the structures of five more beticolins were proposed by comparison of their NMR spectroscopy and mass spectrometry data, and correlated by chemical transformations⁷⁻⁹ with the already determined B0 and B2 (Scheme 1). All the beticolins display structural analogies: they share the same polycyclic skeleton made of two subunits (a partially hydrogenated anthraquinone and a xanthone moiety), and, unusually, they also include a chlorine atom attached to the central aromatic ring. The beticolins are classified into three sub-groups according to (i) the type of cyclisation of the heterocycle, which may occur with the oxygen O(1) being in the *ortho* position with respect to the chlorine atom (*o*-beticolin) or in the *para* position (*p*-beticolin); (ii) the relative configuration of the methoxycarbonyl and the secondary hydroxy substituents at C(2) and C(3) which can be either on opposite (*epi-p*-beticolin) or on the same side (*p*- and *o*-beticolin) of the mean plane of the first ring. The beticolins are the parent structures of a new class of natural compounds, the xanthraquinones, which now encompass the xanthoquinodins described recently.¹⁰

In order to confirm the proposed structures of the *p*-beticolins and to determine the minor compounds present in the extracts, the crystallogenesis conditions for preparing single crystals of beticolins were investigated. This report describes the optimal conditions that afforded single monocrystals suitable for X-ray analysis of the three *p*-beticolins. As only microcrystals were obtained, the X-ray diffraction studies were only possible using the powerful X-ray source of a synchrotron

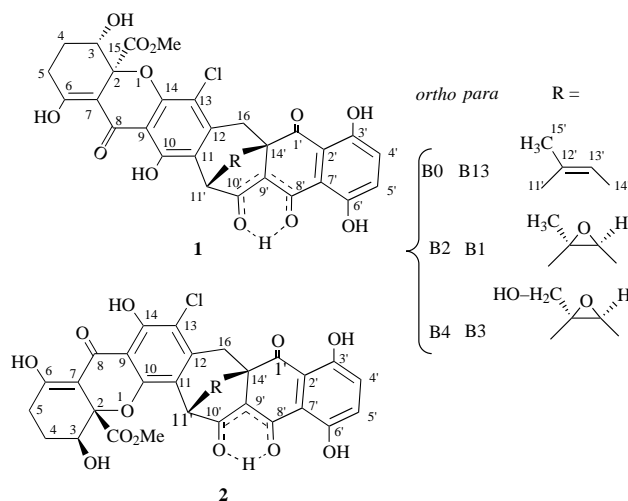


Fig. 1 Structures of *o*-beticolins **1** and *p*-beticolins **2**. Atoms are labelled in *p*-beticolin according to their original position in the *ortho* subgroup resulting from their chemical transformation (B0→B13, B4→B3 and B2→B1), following the rearrangement given in Scheme 1.

beam line. This allowed us to confirm the proposed structures of B1 and B3 and to elucidate the structure of B13.

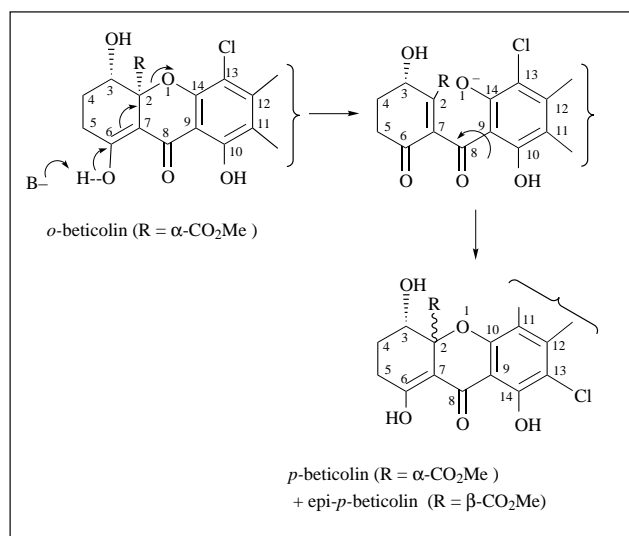
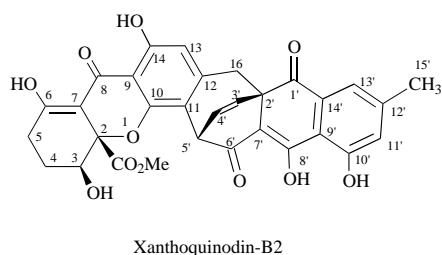
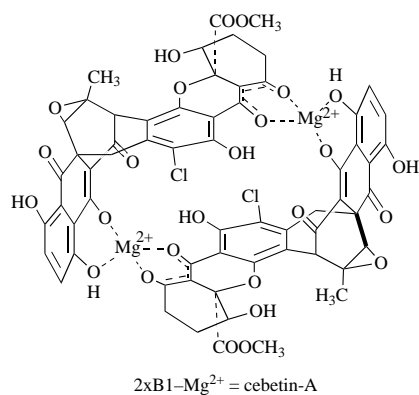
Results

Crystallisation aspects

Compared to the *o*-beticolins (B0, B2 and B4) (Fig. 1), the isomeric *p*-beticolins (B13, B1 and B3), displayed very poor crystalline properties. When submitted to crystallisation in the same conditions, they gave only microcrystalline precipitates.

We made use of the fact that beticolins are polyaromatic compounds with donor-acceptor properties in the presence of various aromatic solvents such as anisole, benzene or chlorobenzene. We focused our attention on anisole as a possible donor in charge transfer complex formation with the *p*-beticolin subgroup in the hope of forming ordered species that could be crystallised as charge transfer species or as solvate complexes. The observation that *p*-beticolins were very soluble in anisole and much less soluble in benzene or toluene was encouraging for the application of the vapour diffusion technique already developed in protein crystallography. In our case, anisole was the solvent and toluene (the less polar counterpart)

* E-Mail: prange@lure.u-psud.fr; Fax: 33 1 48 38 77 77.



Scheme 1 Rearrangement of *o*- to *p*-beticolins in basic media (boxed) and the molecular structures of cebetin (top) and xanthoquinodins (bottom)

was the precipitant. The use of the diffusion vapour technique gave, over a period of several weeks at 4 °C, bright yellow microcrystals. These crystals were, at least in the case of B1 and B3, unstable when harvested from the solvent and it was necessary to mount them in flame-sealed Lindeman capillaries in the presence of the mother liquor to avoid any decomposition of the crystal lattice. The crystals of B13 were more stable, at least over a period of a week at room temperature, when removed from their mother liquor. In the case of B3, limited success was achieved: crystals were characterised as very small plates of less than 10 μ m thickness.

All the beticolins were very sensitive to light and heat when they were in solution prior to crystallisation. They slowly decomposed during the crystallisation processes and after one or two attempts, they lost their ability to crystallise and had to be re-purified, when this was possible.

X-Ray diffraction experiments

We have shown previously^{4,5} that all the *o*-beticolins that have been crystallised give crystals with the same orthorhombic

$P2_12_12_1$ space group, with very similar parameters and that are isomorphous. The asymmetric unit contains one independent, non-solvated molecule. In contrast, the *p*-beticolins crystallised as dimer complexes in monoclinic systems, usually solvated with anisole.

The crystal data of the *p*-beticolins are reported in Table 1. There is one molecule of anisole per molecule of B1 in the lattice (two anisoles per dimer in the asymmetric unit or a 1:1 stoichiometry), but only one anisole molecule per dimer was found in the case of B13 (2:1 B13-solvate), and two anisoles per four molecules of B3 (2:1 B3-solvate). Beticolin-1 crystallised as small elongated prisms in the $C2$ space group. Beticolin-3 was obtained as very small crystals, 0.2 \times 0.15 \times 0.01 mm, which are unsuitable for standard diffractometers. They were characterised at the LURE synchrotron facility in Orsay (France) as a close primitive form of beticolin-1, in the $P2_1$ space group instead of $C2$, with the same number of molecules in the cell ($Z = 8$, or two independent dimers). Beticolin-13 was obtained in two different crystal habits, depending on the crystallisation batches, resulting from competing complexation of either anisole or chlorobenzene, the two solvents used in the experiments. Although they have closely related axis lengths and angles, these two forms have completely different packings and are not isomorphous. The first form (B13A) gave crystals big enough to be recorded on a standard diffractometer but the second crystalline form (B13B) was obtained only as microcrystals. B13B was recorded at the DCI synchrotron source in LURE, Orsay, France (Table 1). The only difference observed between the two cells was the nature of the unique solvated molecule observed in the packing: chlorobenzene in B13A and anisole in B13B.

Discussion

Beticolin-1

The molecular packing was found to be rather loose with only a few hydrogen bonds between the dimers, accounting for the poor quality and stability of the crystals. In addition to the two well-defined anisole molecules, two strong peaks were interpreted as water molecules in the final model. The X-ray analyses confirmed the proposed structure for B1⁷ which corresponds to the monomer of the magnesium complex previously determined by Jalal *et al.*⁶ and which was also confirmed a year later by Arnone *et al.*¹¹

Beticolin-3

The crystals were very small and the diffraction data could only be measured up to 1.25 Å resolution. The asymmetric unit contains four units of B3 (a dimer of a dimer) and shows a pseudo-I-centred cell, with about 80% of the odd $h + k + l$ reflections weak or unobserved. It was not possible to solve the structure easily by direct methods with this limited resolution and molecular replacement techniques were employed successfully. The electron density (calculated with the refined phases) is given in Fig. 2, superimposed on the molecular model. B3 differs from B1 at C(15') (hydroxymethyl instead of a methyl group).

Beticolin-13

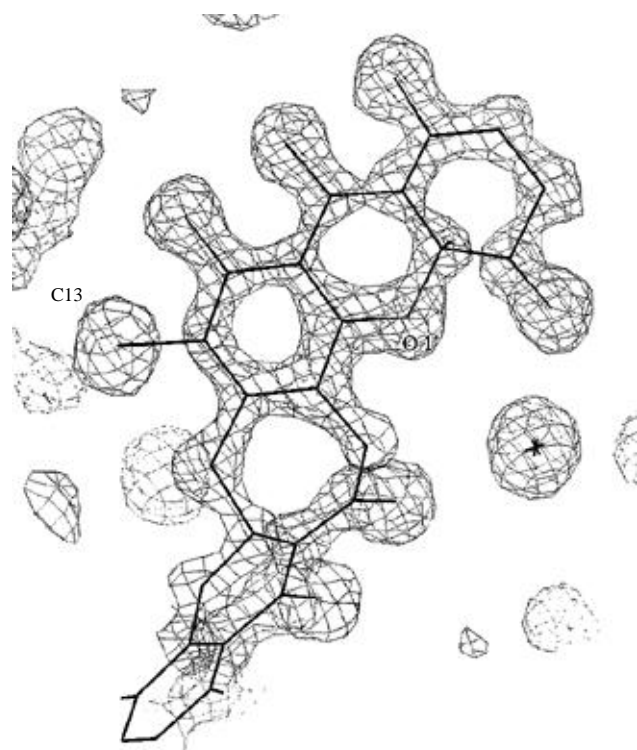
By comparing the NMR data of B13 with that of B1, a deoxy structure was proposed. B13 could also be obtained by transformation of B0 in polar solvents. The X-ray determination confirms that B13 is the corresponding de-epoxidated derivative of B1. Fig. 3(a) represents the ORTEP view¹³ of one monomer of B13 with ellipsoids drawn at the 50% probability level.

General features of the *p*-beticolins

Like the *o*-beticolins, the *p*-beticolins are very rigid molecules. The least-squares fit of all the molecules is given in Fig. 4(a) for the three available *o*-beticolins (B0, B2 and B4) and in Fig. 4(b) for all the different monomers (2 \times B1, 4 \times B3, 2 \times B13A and

Table 1 Crystal data for the *p*-beticolins, B1, B3 and B13

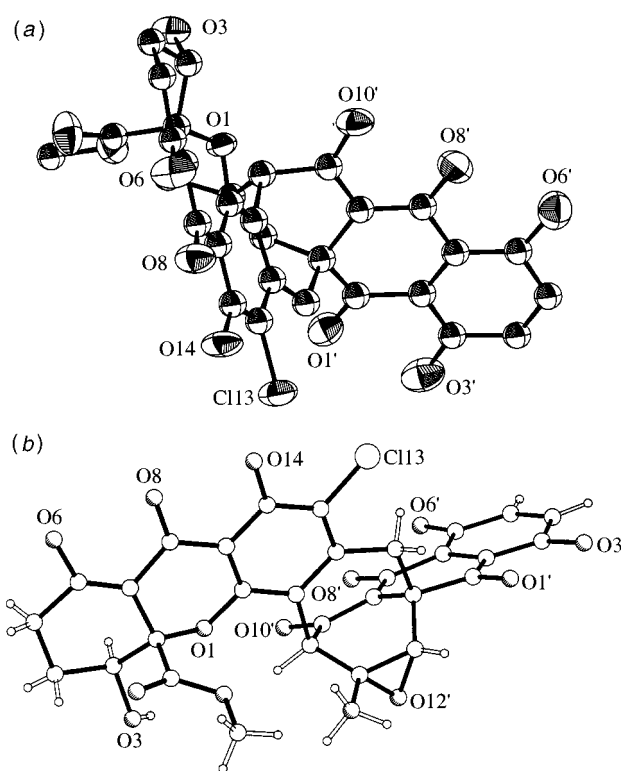
	Compound (X-ray instrument)			
	B1 (Diffractometer)	B3 (LURE)	B13A (Diffractometer)	B13B (LURE)
Chemical formula	C ₃₁ H ₂₃ ClO ₁₃	C ₃₁ H ₂₃ ClO ₁₄	C ₃₁ H ₂₃ ClO ₁₂	C ₃₁ H ₂₃ ClO ₁₂
<i>M_w</i>	638.97	654.97	622.97	622.97
No. of independent molecules	2	4	2	2
Solvent	2 Anisoles, 2 waters	2 Anisoles, 1 water	1 Chlorobenzene	1 Anisole
Space group	<i>C</i> 2	<i>P</i> 2 ₁	<i>P</i> 2 ₁	<i>P</i> 2 ₁
Cell parameters, <i>a</i> /Å	23.943(4)	19.331(4)	16.261(3)	16.391(5)
<i>b</i> /Å	16.040(4)	16.030(4)	20.302(4)	20.172(5)
<i>c</i> /Å	19.866(5)	22.880(4)	9.393(3)	9.380(3)
β /°	117.5(1)	110.1(1)	105.39(8)	107.83(7)
Volume/Å ³	6766.7	6658.1	2989.6	2952.9
Wavelength/Å	1.5418	0.980	1.5418	0.980
μ /mm ⁻¹	1.68	0.20	2.15	0.20
<i>F</i> (000)	3184	3208	1404	1404
No. of independent reflections	6403	3979	3874	2909
No. of reflections in the refinement	5128	3087	2714	2867
No. of independent atoms	108	201	95	96
No. of missing hydrogens in the refined models	16	48	24	12
No. of parameters	973	825	511	865
Thermal factors in refinement	All anisotropic	Cl Anisotropic C, O isotropic	Cl, O Anisotropic C isotropic	All anisotropic
<i>R_w</i> 2 on <i>I</i> %	0.222	0.285	0.220	0.179
<i>R_w</i> 1 on <i>F</i> %	0.079	0.111	0.08	0.067
Min/Max in last difference-Fourier map/e Å ⁻³	-0.4/+0.3	-0.7/+0.4	-0.35/+0.3	-0.3/+0.25

**Fig. 2** Part of the electron density of B3 with the refined molecular model (contouring at the 2σ average density level) at a resolution of 1.25 Å (synchrotron data)

2 × 13B) superimposed on one another. They are almost identical in shape and form, with rms deviations in the range of 0.15–0.3 Å for all the atoms (except the C12'–C13' variable bridge which was removed from the calculations).

The overall V molecular shape of the *o*-beticolins⁴ is no longer observed in the *p*-beticolin subgroup where the shape turns out to be a linkage of two planes, roughly perpendicular to each other. This is clearly visible in Fig. 5.

Compared to the *o*-beticolin [Fig. 4(a)], the overall shape of the *p*-beticolins [Fig. 4(b)] is completely different and is one of the remarkable features that encourages the *p*-beticolin to form

**Fig. 3** (a) ORTEP drawing of one monomer of B13, with the ellipsoids drawn at the 50% probability level, as determined from synchrotron radiation on microcrystals. Hydrogens are not included. (b) PLUTO representation of one element of the B1 structure. The localised hydrogens are represented in light tracing.

dimers by complexing magnesium cations with a high affinity.¹² In the absence of Mg²⁺, however, they retain the ability to form dimers as shown in Fig. 5, which depicts the dimeric arrangement of beticolin-13 crystals even when no magnesium is present (the solvated anisole is removed from the figure for clarity).

Dimeric packing

o- and *p*-Beticolins possess delocalised β -keto-phenol groups that permit, at least in the case of the *p*-beticolins, the chelation

Table 2 Intra- and inter-molecular non-bonded contacts in the packing structures of B1, B3 and B13B

B1			B3			B13B		
Atoms ^a	Sym. op ^b	Dist./Å	Atoms ^a	Sym. op ^b	Dist./Å	Atoms ^a	Sym. op ^b	Dist./Å
O10'B-Ow2'B	[1 000] [1 000]	2.81	O3A-Ow1	[1 000] [1 000]	2.74	O6A-O6'B	[1 000] [1 000]	3.22
O14A-O10'B	[1 000] [1 000]	3.25	O10'A-Ow1	[1 000] [1 000]	2.94	O8A-O8'B	[1 000] [1 000]	3.10
			O15B-O12D	[1 000] [1 000]	2.98	O14A-O10'B	[1 000] [1 000]	3.30
O3B-O3B	[1 000] [2 001]	2.60	O14B-O10'D	[1 000] [2 101]	3.03	O3A-O3B	[1 000] [1 001]	2.85
O3A-Ow1	[1 000] [2 101]	2.81	O8'B-Os1	[1 000] [2 101]	2.97	O10'A-O3'B	[1 000] [1 -100]	3.09
O14A-Ow1	[1 000] [2 101]	2.98	O10'B-Ow1	[1 000] [2 101]	2.97	O6'A-O14B	[1 000] [2 1 -10]	3.01
O3B-Ow2	[1 000] [2 001]	3.02	O8B-O1'D	[1 000] [1 100]	3.09	O6'A-O8B	[1 000] [2 1 -10]	2.80
O6A-O6'A	[1 000] [3 0 -10]	3.04	O3C-O3D	[1 000] [2 101]	2.77	O3A-O14A	[1 000] [1 001]	3.08
O8A-O1'B	[1 000] [4 0 -11]	3.06	O3B-Ow1	[1 000] [2 101]	2.83			
O8'A-Os1	[1 000] [3 -100]	3.08	O3C-O15D	[1 000] [2 101]	2.65			
			O15'C-O3D	[1 000] [2 101]	2.78			

^a Letters A and B (or A-D) refer to the subunits within a given dimer (or tetramer), Ow and Os are the water and anisole oxygens of the solvated molecules. ^b Symmetry operations given as usual: the first number is the operation as in the *International Tables for X-Ray Crystallography* (vol. I), (Kynoch Press, Birmingham, 1974), followed by the three translations along the crystallographic axes.

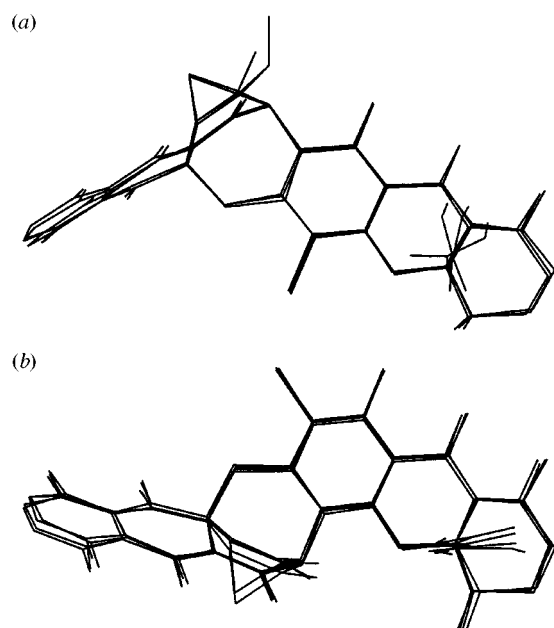


Fig. 4 Least squares fits (LSQ) of all the (a) *o*-beticolin and (b) *p*-beticolin structures using the BMF program, showing the structural differences between the two subgroups, and also the similarities within each subgroup

of a divalent cation (e.g. Mg^{2+} , Co^{2+} and Mn^{2+}). The natural dimer (Mg^{2+}) of the *p*-beticolins is built in a head-to-tail fashion around two cations through complexation of the two keto-enol systems of each monomer (Scheme 1). This allows the building of asymmetric complexes with a central two-fold axis, since the two β -keto-enol groups are located on both sides of the molecule: O(6)-C(6)-C(7)-C(8)-O(8) in the xanthone and O(6')-C(6')-C(7')-C(8')-O(8') in the anthraquinone. In the case of *o*-beticolins, only one delocalised system is observed,⁴ in which the unfavourable geometry and the lack of the second delocalised β -keto-enol group on the opposite side prevent the head-to-tail dimerisation.

In the uncomplexed dimers of *p*-beticolins (Fig. 5) it may be noted that (i) the second delocalised system, including O(6') and O(8') of the anthraquinone, is a classic diphenol system and again, as in *o*-beticolins, the delocalisation is displaced one step ahead, on C(10') C(8'), as indicated in Fig. 1 and (ii) the overall dimer structure is retained and the association of the two monomers mimics the magnesium complex through hydrogen bonds. However, the two-fold molecular symmetry is no longer possible as the two molecules are shifted with respect to

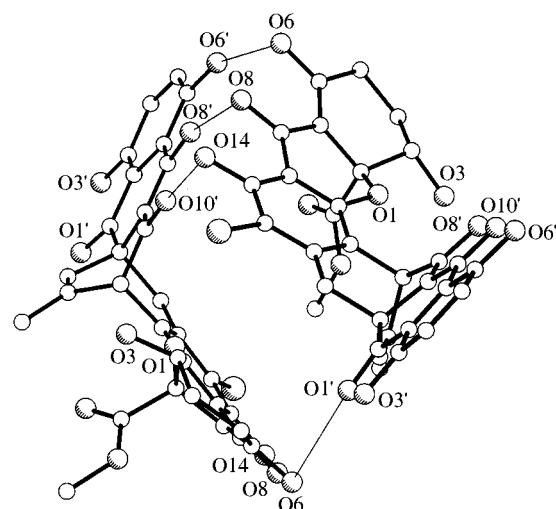


Fig. 5 View of the molecular dimer built by the two subunits in the B13 structure. The two independent molecules assemble themselves by hydrogen bonding, mimicking the magnesium chelate observed in cebetin-A, except that no magnesium is present here.

each other to ensure formation of the dimer without a chelating agent. As the two elements of the dimer are now closer to each other, this leads to a dissymmetry in the hydrogen bond networks: three strong H bonds are observed on one side, but only one very weak interaction on the other side, which is directed towards O(3) of molecule 2, crossing over the xanthone plane (Fig. 5). Fig. 5 also shows that the O(6'), O(8') and O(10') atoms of molecule 2 are not free; they are involved in intermolecular hydrogen bonding with another dimer in the packing (not shown), towards the O(6), O(8) and O(14) of another intermolecular molecule 1. This infinite H-bond network [. . . molecule 1_n → molecule 2_n → molecule $1_{(n+1)}$ → . . .] explains the relative stability of the *p*-beticolin crystals (Table 2).

Role of the solvated anisole

The solvent of crystallisation is part of the crystal lattices in all the beticolins. It was initially presumed that if they were present, the anisole molecules would be involved in strong stacking interactions with the anthraquinone ring of the beticolins. The X-ray structures reveal that, if anisole molecules have a clear visible signature in the crystal packing, they have essentially no stacking contacts with the beticolin quinone or phenol rings. The anisole molecules just fill empty spaces in the lattices giving an anisole-beticolin ratio of 1:1 (beticolin-1) or 1:2 (beticolins-3 and -13). As a result of their loose constraints, these solvent molecules display quite high thermal factors. In

the particular case of B13, a mixture of chlorobenzene-anisole was used for the crystallisations. As mentioned earlier, two different forms were obtained: the first was found to contain a molecule of anisole and the other, a disordered molecule of chlorobenzene.

Absolute configuration and the biosynthesis of beticolins

The atom numbering of the beticolins is given in Fig. 1, which has been deduced from the chemical rearrangement of the *ortho* to the *para* subgroup by opening of the heterocyclic ring followed by a rotation around the C(9)–C(10) bond and ring closure (Scheme 1). This implies that the chiral centres are not affected, except at C(2). This inversion allows the hydroxy group at C(3) to be equatorial instead of axial and the chlorine atom is attached to the *para* position with respect to O(1). There is still a question about the order of the biosynthesis steps, being either (i) two distinct assemblies of the two moieties as outlined previously,⁴ followed by chlorination at the free position, C(13) or C(11) or (ii) the *o*-beticolins may be formed as precursors, followed by an enzyme-acid-base catalysed interconversion mechanism to give the more stable *para* subgroup.

The latter hypothesis is strongly supported by the facile chemical transformation⁹ of the *ortho* to the *para* subgroup in mild basic media (MgCO₃) by ring opening or with polar solvents. An equivalent equilibrium has been observed in the case of xanthoquinodins.¹⁰ This hypothesis is also supported by the isolation of both the resulting *p*-beticolin and its *ortho* precursor in the same mycelial extract.

It should also be noted that, with the exception of C(2), the absolute configuration of the chiral centres should not be modified. Two attempts were made to determine the absolute configuration of beticolins by X-ray diffraction.^{4,6} Despite the weakness of the anomalous contribution of the single chlorine atom ($\Delta f'' = +0.702e^-$ and $\Delta f' = +0.348e^-$ at $\lambda = 1.5418 \text{ \AA}$) it is possible to reach a conclusion about the absolute configuration. In one experiment, using the best crystal available (*o*-beticolin B2), the complete sphere of diffraction data was re-recorded. Both *hkl* and the associated Friedel $\bar{h}\bar{k}\bar{l}$ reflections were measured successively. The Flack *x* index,¹⁴ as coded in the SHELXL93 refinement program¹⁵ was used in the final stages of the refinement to determine the correct absolute configuration. The *x* value must be close to zero (within deviation of 3σ) for the correct configuration and close to unity for the wrong one. The values obtained (with esds in parentheses) were 0.83 (0.08) and 0.167 (0.08), respectively, for the two configurations, thus giving a clear indication that the second solution is the correct configuration (shown in Fig. 1). Consequently, in *o*-beticolins, the chiral centres are C(2): *R*, C(3): *S*, C(11'): *R*, C(12'): *R*, C(14'): *S*.

Determination of the absolute configuration of *p*-beticolins is less straightforward because the crystals are all of bad quality and somewhat mosaic, so the accuracy of the results is less certain, though the Flack index gives reasonable correlation. The most accurate recordings were made using the LURE synchrotron facility, but the wavelength used is monochromated around 0.9 Å, a value at which the chlorine atom essentially makes no contribution to the anomalous diffraction. Circular dichroism (CD) was then employed to correlate the *o*- and *p*-beticolin subgroups.

In the past, chiral molecules bearing two strong coupled chromophores, well oriented with respect to each other, have been studied intensively by CD.¹⁶ This technique, based on the coupling harmonic oscillator theory, is a complementary method to X-ray diffraction for determining absolute configurations.¹⁷ Beticolins are examples of this type of molecule as they include two individual systems: an anthraquinone and the chloro-dien-one system of the xanthone moiety.

The orientations of the two electric moment transition vectors, although difficult to evaluate, can be estimated from the X-ray coordinates. This would allow an evaluation of the chirality,

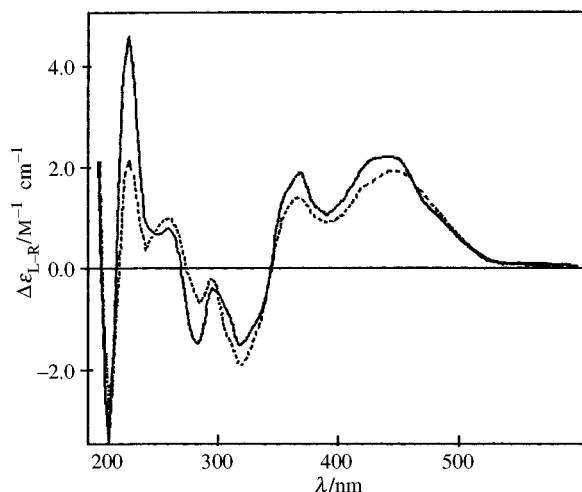


Fig. 6 Superimposed CD spectra of the two generic *o*- (B2, ---) and *p*-beticolins (B1, —)

based on the sign of the calculated Cotton effects. The CD spectra for the two parent structures B2, *o*- and B1, *p*-beticolin subgroups are given in Fig. 6. These spectra are nearly equivalent, particularly in the domain corresponding to the anthraquinone chromophore (300–400 nm) where a broad positive doublet of couplet is observed. In the absence of reliable rules, this Cotton effect cannot be used directly for an unambiguous determination of the absolute configuration itself. However, this equivalence in the CD spectra suggests that *o*- and *p*-beticolin share the same absolute configuration of the anthraquinone system.

It is therefore possible to conclude that the absolute configurations of *p*-beticolins are identical to that of the *o*-beticolins, except at C(2) which has an *S* configuration. An equivalent conclusion was independently reached by Jalal *et al.*⁶ in the case of cebetin-A.

Conclusions

The molecular structures of three *p*-beticolins were determined on microcrystals with the aid of a synchrotron radiation source and their absolute configurations were established by correlation with the *o*-beticolins, whose structures have also been previously obtained by X-ray diffraction analyses but using different crystallogensis conditions.^{4,5} New techniques for crystallising and recording the X-ray diffraction data have been developed to carry out this study.

In addition to the *o*- and *p*-beticolins, several other, closely related, yellow derivatives were also extracted from *C. beticola*. Their structures, which have not yet been correlated with either the *ortho* or the *para* subgroup, are currently under investigation.

Experimental

The culture of *Cercospora beticola*, purification and separation of beticolins from the mycelial extracts have already been published.¹⁸

CD Spectra

Spectra were recorded on a Jobin Yvon Mark II Dichrograph spectrometer, interfaced with an Apple II computer, using 1 cm cell paths and concentrations of $2 \times 10^{-4} \text{ M}$ (in methanol).

Crystallisations

Crystallisations were carried out by the sitting drop method in nine well Dow Corning plates in groups of three wells with the plate ground flat to permit sealing with standard microscope slides and with the central well in each group connected to the two flanking wells by a notch cut in the glass. Each three-well

Table 3 X-Ray data processing details

	Beticolin			
	B1	B3	B13A	B13B
Recording method	A	B	A	B
Crystal size/mm	0.4 × 0.2 × 0.1	0.2 × 0.5 × 0.01	0.3 × 0.1 × 0.05	0.2 × 0.15 × 0.01
Max. resolution/Å	0.9	1.25	0.85	1.05
No. of scanned reflections	9201	12 236	3228	16 928
No. of independent reflections	6933	3979	2927	2909
R_{symm} (%) on intensities	4.5	8.5	7.7	4.5
No. of observed reflections ($\geq 4\sigma$)	6403	3214	2427	2875
Absorption corrections ($T_{\text{min}}/T_{\text{max}}$)	0.76/1.3	—	0.82/1.22	—

group thus forms a microdiffusion chamber suitable for reverse vapour diffusion by placing the precipitant solution (here 2 ml of toluene) in the central well and the crystallisation solution (usually 2–4 mg of beticolin in a 100 μ l anisole solution) in the flanking wells. Bright yellow micro platelets were obtained at 4 °C after a period of one or two weeks.

B1 and B3 crystals gave unstable crystals when removed out of the mother liquor: they were mounted in Lindeman capillaries (0.3 mm in diameter) and flame sealed at both ends. B13 crystals were stable enough to be manipulated out of the solvent, at least for a week.

Data recordings

Method A. The diffraction data were recorded on a four-circle PHILIPS PW1100 diffractometer operating with the Cu-K α radiation ($\lambda = 1.5418$ Å), monochromated by graphite. The diffraction data were recorded in the (ω - 2θ) step-scan mode up to $2\theta = 130^\circ$ (30 steps per scan over a scan angle of 1.2° for each reflection). They were processed and corrected in structure amplitudes as usual using a profile-fitting program (Table 3).

Method B. A microcrystal of B13 was glued on top of a thin glass fibre ($\phi < 10$ μ m), which was itself secured into a thicker hollow glass fibre ($\phi > 0.1$ mm). It was mounted on a conventional goniometer head and fitted to a MAR Research 32 cm diameter Image-Plate system, connected to the W32 beam line station, LURE-DCI synchrotron, in Orsay (France), monochromated by a silicon(111) bent crystal and focused in the other direction using a multi-layered mirror.¹⁹ The wavelength used was 0.91 Å. Each frame consists of a 5° rotation of the crystal (randomly oriented along the spindle axis) recorded in 30 s exposure time. The overall angular domain was 270° . The image-plate-to-crystal distance was kept as small as possible (1.01 Å at the edge of the plate) in order to get the highest possible resolution. The orientation matrix and cell parameters were determined using the IMSTILLS and REFIX programs.²⁰ The intensities were processed by profile-fitting with MOS-FLM²¹ and the data reduction performed with the ROTAVATA and AGROVATA programs from the CCP4 suite of programs.²² The overall time period used in this over-redundant data collection was less than 4 h, in contrast to the diffractometer data which needed more than a week for completion of a single asymmetric unit. B3 crystal data were measured in the same way but they were mounted in sealed capillaries.

Structure determinations

Beticolin-1. The dimeric structure corresponds to more than 100 independent atoms. Some difficulties were encountered in the structure determination by direct methods. The best solution was selected according to the highest negative value of the quartet test²³ after several attempts and hand-optimisation of the input parameters. In the E-map calculated with the resulting phases it was possible to localise most of the two independent molecules, one anisole was also easily observed. Eleven atoms were missing in the peak list. They were located in successive Fourier-difference syntheses. In addition, two water molecules

were also located and their contribution added to the atomic model.

Beticolin-3. Due to the limited diffraction (1.25 Å) and the number of independent atoms (≈ 200) that needed to be localised, direct methods were not even attempted. The structure was solved by the molecular replacement method, using the AMoRe program²⁴ at a limited range of resolution between 4 and 1.5 Å. The four correct orientations of the model (a monomer taken out from the previously solved B1 structure) were determined in a straightforward manner. The translation step was more difficult to tackle. This was achieved with the phased translation option implemented in the program. The four oriented/translated molecules were determined in the same run, refined as rigid models (final correlation coefficient = 89% and R factor = 31%). The structure was refined by successive cycles of full-matrix least squares refinements (with individual isotropic factors), followed by Fourier-difference map calculations. The missing atoms [the four O(15') oxygens, with respect to the initial model of B1] were immediately located on the first $|F_o - F_c|$ map as the four highest peaks. A round shaped density (see Fig. 2) was observed at the correct bond distance and angle for a hydrogen bond. It was attributed to a solvated molecule of water. Two anisole molecules were also located during the next cycles. In the last cycles of refinements, only the chlorine atoms were assigned anisotropic thermal parameters.

Beticolin-13. The structure was easily solved by direct methods²³ for both B13A and B13B. This was quite straightforward for B13B (LURE data) but realised with some difficulties in the case of B13A (successive E recycling procedures were necessary to obtain the whole set of atoms). The diffractometer data were found to be much noisier when compared to the LURE data, although the crystals were bigger. The two structures B13A and B13B are not isomorphous (the R_{iso} between the two data sets is greater than 30%). These are two different arrangements in a similar cell.

The refinements were made using the SHELXL93 program.¹⁵ A first round of full matrix least squares refinements were carried out using isotropic thermal parameters. Hydrogen atoms, when it was possible, were put at their theoretical places with an isotropic temperature factor equal to that of the bonded atom. At the end of the isotropic refinement, an empirical absorption correction was applied²⁵ for B1 and B13A (recorded at Cu-K α , $\lambda = 1.5418$ Å); the minimum and maximum corrections to the diffraction data are reported in Table 3.

The refinements were continued with anisotropic thermal parameters for the non-hydrogen atoms for B1 and B13B, and with mixed anisotropic/isotropic thermal parameters in the case of B13A and B3, due to the limited amount of data.

Atomic coordinates, thermal parameters and bond lengths and angles have been deposited at the Cambridge Crystallographic Data Centre (CCDC). See Instructions for Authors, *J. Chem. Soc., Perkin Trans. 2*, 1997, Issue 1. Any request to the CCDC for this material should quote the full literature citation and the reference number 188/78. They can also be obtained as standard .cif files by e-mail to the following address: prange@lure.u-psud.fr.

Acknowledgements

We express our thanks to the Action Concerté du Vivant (ACCSV n°5) from MENESR/CNRS and Conseil Régional de Bourgogne for financial support, Drs J. Einhorn, P. H. Ducrot and C. Descoins for their interest and Dr Javier Perez for access to the LURE synchrotron W32 beam line. We also warmly thank J. Navaza for his advice on the use of AMoRe in our unusual conditions at high resolution.

References

- 1 S. Kuyama and T. Tamura, *J. Am. Chem. Soc.*, 1957, **79**, 5725.
- 2 E. Schlösser, *Phytopathol. Mediterr.*, 1971, **10**, 154.
- 3 M. L. Milat, T. Prangé, P. H. Ducrot, J. C. Tabet, J. Einhorn, J. P. Blein and J. Y. Lallemand, *J. Am. Chem. Soc.*, 1992, **114**, 1478.
- 4 T. Prangé, A. Neuman, M. L. Milat and J. P. Blein, *Acta Crystallogr., Sect. B*, 1995, **51**, 308.
- 5 P. H. Ducrot, J. Einhorn, L. Kerhoas, J. Y. Lallemand, M. L. Milat, J. P. Blein, A. Neuman and T. Prangé, *Tetrahedron Lett.*, 1996, **37**, 3121.
- 6 M. A. F. Jalal, M. B. Hossain, D. J. Robeson and D. Van der Helm, *J. Am. Chem. Soc.*, 1992, **114**, 5967.
- 7 P. H. Ducrot, J. P. Blein, M. L. Milat and J. Y. Lallemand, *J. Chem. Soc., Chem. Commun.*, 1994, 2215.
- 8 M. L. Milat, J. P. Blein, J. Einhorn, J. C. Tabet, P. H. Ducrot and J. Y. Lallemand, *Tetrahedron Lett.*, 1993, **34**, 1483.
- 9 P. H. Ducrot, J. Y. Lallemand, M. L. Milat and J. P. Blein, *Tetrahedron Lett.*, 1994, **35**, 8797.
- 10 N. Tabata, H. Tomoda, K. Matsuzaki and S. Omura, *J. Am. Chem. Soc.*, 1993, **115**, 8558.
- 11 A. Arnone, G. Nasini, L. Merlini, E. Ragg and G. Assante, *J. Chem. Soc., Perkin Trans. 1*, 1993, 145.
- 12 V. Mikes, S. Lavernet, M. L. Milat, E. Collange, M. Pâris and J. P. Blein, *Biophys. Chem.*, 1994, **52**, 259.
- 13 C. K. Johnson, ORTEP-II report ONRL-5138, Oak-Ridge National Laboratory, USA, 1976.
- 14 G. Bernardinelli and H. D. Flack, *Acta Crystallogr., Sect. A*, 1985, **41**, 500.
- 15 G. M. Sheldrick, *SHELXL-93, program for the refinement of crystallographic structures*, University of Gottingen, Germany, 1993.
- 16 N. Harada and K. Nakanishi, in *Circular dichroism spectroscopy—Exciton coupling in organic chemistry*, University Science Books, Mill Valley, 1983.
- 17 S. F. Masson, in *Molecular optical activity and the chiral discriminations*, Cambridge University Press, Cambridge, London, New York, 1982.
- 18 M. L. Milat and J. P. Blein, *J. Chromatogr.*, 1995, **A699**, 277.
- 19 R. Fourme, P. Dhez, J. P. Benoit, R. Kahn, J. M. Dubuisson, P. Besson and J. Frouin, *Rev. Sci. Instrum.*, 1992, **63**, 982.
- 20 W. Kabsch, *J. Appl. Crystallogr.*, 1988, **21**, 67.
- 21 A. Leslie, *Mosflm User Guide, Mosflm version 5.20*, MRC Laboratory of Molecular Biology, Cambridge, 1994.
- 22 Collaborative Computational Project, Number 4, The CCP4 suite: Programs for protein crystallography, *Acta Crystallogr., Sect. D*, 1994, **50**, 760.
- 23 G. M. Sheldrick, *Acta Crystallogr., Sect. A*, 1990, **46**, 467.
- 24 J. Navaza, *Acta Crystallogr., Sect. D*, 1994, **50**, 157.
- 25 N. Walker and D. Stuart, *Acta Crystallogr., Sect. A*, 1983, **39**, 158.

Paper 6/08511C
Received 19th December 1996
Accepted 22nd April 1997